SAND2013-3047C

Effect of Gamma-Ray Irradiation on the Thermal Contact Conductance of Carbon Nanotube Thermal Interface Materials

Stephen L. Hodson[1,2], Robert A. Sayer[3], Timothy P. Koehler[3], Justin R. Serrano[3], Scott M. Dalton[4] and Timothy S. Fisher[1,2]

[1]Birck Nanotechnology Center
Purdue University
West Lafayette, IN

[2]School of Mechanical Engineering
Purdue University
West Lafayette, IN

[3]Engineering Sciences Center
Sandia National Laboratories
Albuquerque, NM

[4]Microsystems Science, Technology & Components Center
Sandia National Laboratories
Albuquerque, NM

Abstract

Thermal interface materials (TIMs) serve a critical role in the thermal management of electronic systems by enhancing the flow of heat from source to sink. Nanostructured materials, such as arrays of carbon nanotubes (CNTs) have been shown to outperform many commercially available TIMs due to their low intrinsic resistance and large compliance that enables them to conform to rough surfaces. These characteristics, combined with their low density and ability to withstand vacuum environments and extreme temperatures, make CNT-based TIMs very suitable for space applications. In space, materials are exposed to high doses of gamma radiation due to the lack of an atmosphere to serve as an absorbing medium. With typical design lifetimes of 5 to 10 years or even more, total radiation exposure can be significant and can affect the structure and performance of the TIM. In this work, the potentially adverse effects on the thermal performance of CNT TIMs of gamma-ray irradiation is reported. CNT TIMs were irradiated in a gamma cell at a rate of 250 rad/s to total doses of 50 and 100 Mrad. The thermal interface resistance was measured before and after gamma-ray irradiation using a transient photoacoustic (PA) method at room temperature and a contact pressure of 134 kPa and indicated no adverse effects of gamma-ray exposure on thermal performance.

Introduction

Interfacial transport continues to play a significant role in the development of small-scale devices for a diverse group of applications. In the electronics packaging industry, creating an efficient heat flow path between the microprocessor and heat sink was considered an important design parameter in the *2007 International Technology Roadmap for Semiconductors* [1]. In a review of current commercial thermal interface materials (TIMs) used in electronics packaging, thermal interface resistance at various junctions was considered to be at least 50% of the total thermal resistance from the silicon chip to ambient environment [2]. Because of their low intrinsic thermal resistance relative to the contact resistance at the contact interface and exceptional mechanical strength, vertically aligned CNT arrays have been extensively studied as an alternative to commercially available TIMs. The CNT TIM performance relies on the ability of the CNT array to alleviate the flow of energy (thermal or electrical) through constricted contact regions at the contact interface [3-10]. Additionally, the stability of CNTs in a variety of environments as compared to other common TIMs such as solders and thermal pastes makes them attractive for applications such as high-voltage switching for more efficient power distribution and electric vehicles, powerful microwave electronics for radar and cellular communications, fuel-efficient jet aircraft and automobile engines, photovoltaics, and thermoelectrics.

Systems in space are often exposed to higher levels of radiation, including charged particles and electromagnetic waves, than their terrestrial counterparts due to the lack of the atmosphere to serve as an absorbing medium. Particle radiation has been

shown to drastically affect CNTs [11–13] by forming inter-tube bonds and cross-linking [13]. TIMs are shielded from these radiation sources which are easily absorbed by the external components of a spacecraft,. On the other hand, high-energy electromagnetic waves such as gamma rays penetrate the exterior materials with minimal attenuation thus providing the potential to affect the CNT TIM.

Skakalova *et al*. [14] observed an increase in the Young's modulus and electrical conductivity of single-walled CNT (SWCNT) papers exposed to gamma-irradiation doses of 5, 17 and 50 Mrad. The maximum change was observed for a dose of 17 Mrad, however, the number of data points are too few to draw a concrete conclusion. Guo *et al*. [15] observed a dramatic increase in the I_D/I_G of the Raman spectrum of gamma-ray irradiated multi-walled CNTs (MWCNTs), which was attributed to the large presence of sp^3-hybridized carbon atoms. This is opposite the trend reported by Xu *et al*. [16], who noted an 8% decrease in I_D/I_G for MWCNTs irradiated to 20 Mrad in air, signaling improved graphitic order. However, when the gamma-ray dosing was conducted in epoxy chloropropane a 9% increase in I_D/I_G occurred. Miao *et al*. [17] investigated the effects of dose rate and total dose on the breaking stress and Young's modulus of MWCNT yarns. Gamma-irradiation was found to increase both of these properties, however the majority of the changes occur rapidly at doses below 10 Mrad. Furthermore, dose rate was negligible on the measured results.

In this work, CNT TIMs are exposed to representative doses of gamma radiation in an effort to explore their capabilities in aerospace and deep space exploration applications. In a gamma cell, the CNT TIMs were irradiated at a rate of 250 rad/s to total doses of 50 Mrad and 100 Mrad. The I_D/I_G band ratio of the tubes was tracked using

a Renishaw InVia Raman microscope, and the thermal interface resistances were monitored using a previously developed photoacoustic technique.

Experimental Setup

CNT TIM Fabrication

In manner similar to that described by Xu and Fisher [4], a thermal evaporative system was used to deposit a tri-layer metal catalyst stack consisting of 30 nm Ti, 10 nm Al, and 5 nm Fe on polished intrinsic Si substrates. Vertically aligned CNT arrays of low density were then synthesized in a SEKI AX5200S microwave plasma chemical vapor deposition (MPCVD) system described in detail in previous work [18]. In summary, the growth chamber was evacuated to 1 Torr and purged with N_2 for 5 min. The samples were heated in N_2 (30 sccm) to a growth temperature of 800°C. The N_2 valve was then closed and 50 sccm of H_2 was introduced to maintain a pressure of 10 Torr in the growth chamber. After the chamber pressure stabilized, a 300 W plasma was ignited and 10 sccm of CH_4 was introduced to commence 2.5 minutes of CNT synthesis. The samples were imaged using a Hitachi field-emission scanning electron microscope (FESEM). Figure 1 contains images of the vertically aligned CNT arrays synthesized on Si. The array characteristics possessed average densities of 10^8-10^9 CNTs/mm^2, tube diameters of 30 nm, and heights near 10 μm.

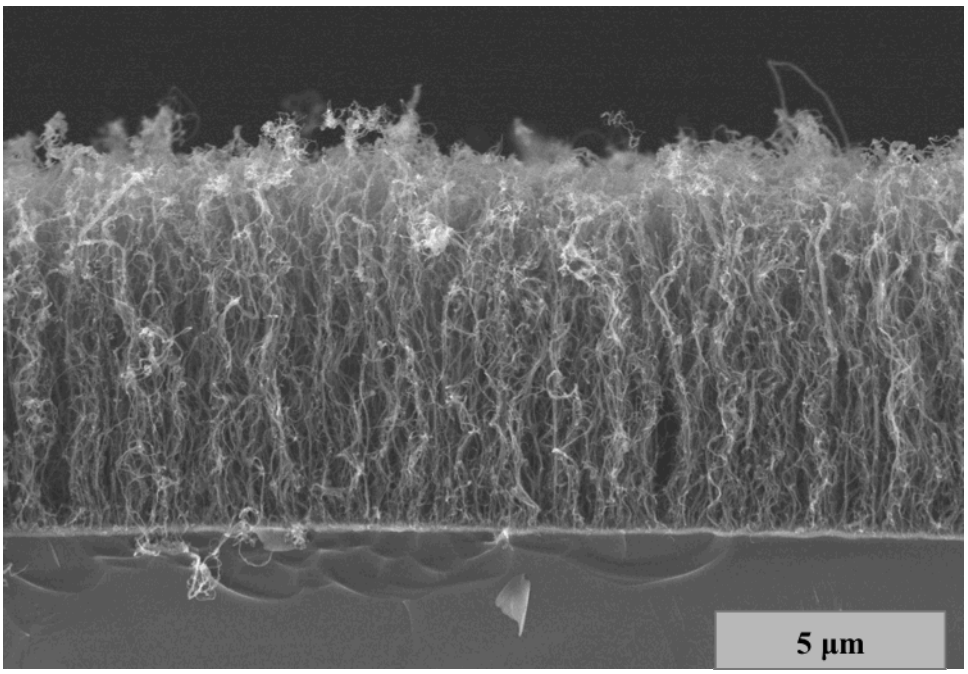

Figure 1. FESEM of CNT TIM grown on Si tab by MPCVD.

Radiation Dosing

Total radiation doses are expected to range between 100 Mrad and 1 Grad at the end of a space mission. For consistency with a previous study, a 10 Mrad radiation dose level per year was assumed as a representative level [19]. Radiation aging of the samples was performed in a gamma cell shown in Figure 2 below. The TIM samples were separated into two bags containing equal numbers of test coupons. The bags were inserted vertically into the test cell together and since the gamma rays penetrated through the materials, no spacing between bags was necessary. The samples were exposed to a gamma ray dose rate of 250 rads/sec for approximately 55 hours to obtain a 50 Mrad dose on each bag. One bag containing three of six samples was removed from the gamma cell, while the second bag was reinserted to the gamma cell for an additional 55 hours to receive a total cumulative 100 Mrad dose of gamma irradiation.

Figure 2. Photograph of test samples in the gamma cell.

Raman Spectroscopy Measurements

Raman measurements were recorded with a Renishaw InVia Raman microscope. The microscope uses a 180° backscattering geometry and a 488 nm Ar+ laser as the probe. The laser is focused by a 20x, 0.40 numerical-aperture objective lens to a ~1 μm diameter spot. The backscattered Raman signal is dispersed by a grating spectrograph and detected by a thermoelectrically-cooled CCS camera with a spectral resolution of 0.95 cm^{-1}/pixel. The power at the sample is limited to ~200 μW to avoid inducing sample heating that would otherwise bias the measurements. Each spectrum was acquired for 110 s.

Thermal Interface Resistance Measurements

A transient photoacoustic (PA) technique that has been described in detail previously [20] was used to characterize thermal interface resistances. Figure 3 contains cross-sectional sketches for each multilayer sample type tested, and Figure 4 shows the experimental setup. For a multilayer structure, the PA technique can resolve both bulk and component resistances in which the bulk resistance in Fig. 3 is defined as

$$R_{bulk} = R_{Si-CNT} + R_{CNT} + R_{CNT-Agfoil} \quad (1)$$

where R_{CNT} is the resistance of the CNT array and $R_{Si\text{-}CNT}$ and $R_{CNT\text{-}Agfoil}$ are the contact resistances at the Si-CNT and CNT-Ag interfaces, respectively [8]. In this work, the bulk thermal resistance was measured. Briefly, in a given PA measurement the sample surface is surrounded by a sealed acoustic cell that is pressurized with helium. The sample is then heated over a range of frequencies by a 350 mW, modulated laser source. The thermal response of the multilayer sample induces a transient temperature field in the gas that is related to cell pressure. A microphone housed in the chamber wall measures the phase shift of the temperature-induced pressure response in the acoustic chamber and the signal is then directed to a lock-in amplifier. Using the acoustic signal in conjunction with the model developed in Ref. 8, which is based on a set of one-dimensional heat conduction equations, thermal interface resistances are determined using a least-squares fitting method.

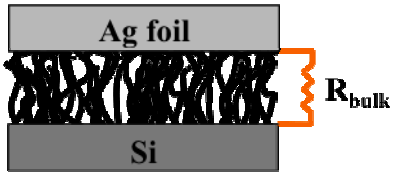

Figure 3. Cross-section of CNT TIM on Si tab for PA testing.

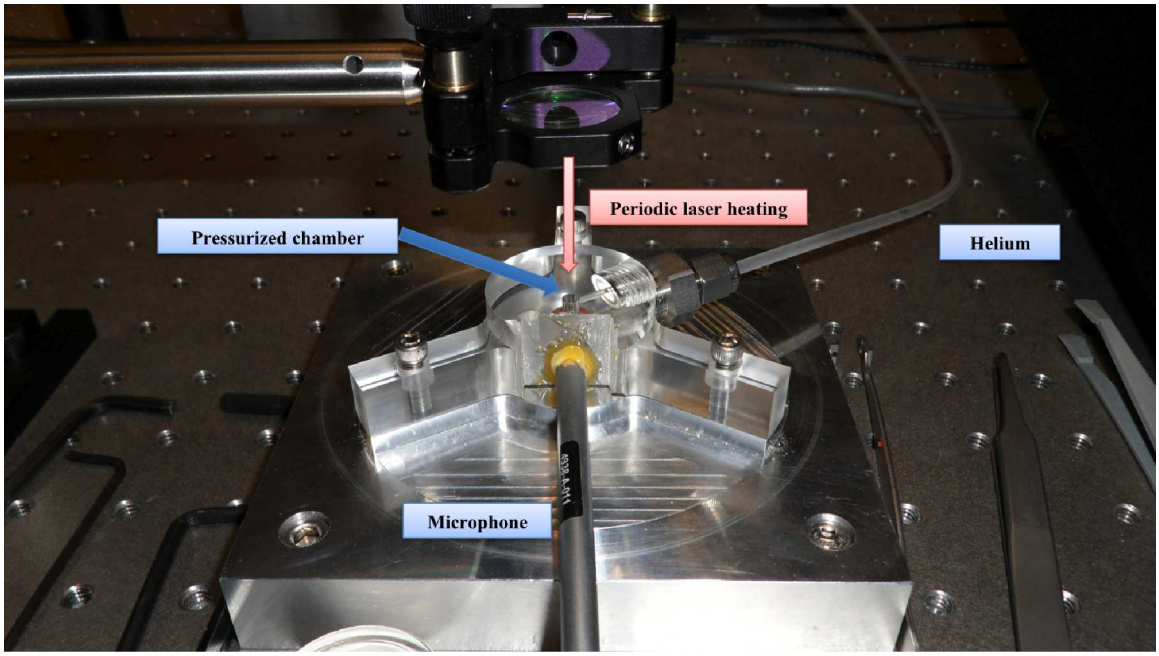

Figure 4. Photoacoustic experimental setup.

Results and Discussion

Raman spectra for every sample were collected at several locations on the sample surface. For all samples and locations the Raman spectra show the presence three distinct spectral features, as shown in Figures 5(a) and (b): the D-peak at ~1360 cm^{-1}, G-peak at ~1585 cm^{-1} and a small peak at ~1620 cm^{-1}. The G-band feature is associated with the E_{2g} optical phonon modes in graphene, while the D-peak is related to vibrational modes associated with the edges of the graphene structure and therefore its presence indicates disorder [21]. The latter D' peak is related to finite-size effects in the CNT [22]. To evaluate the impact of the radiation damage to the CNT films, the ratio of the intensities of the D and G peaks monitored before and after irradiation, as it is a useful indicator of long range order in carbon structures [21].

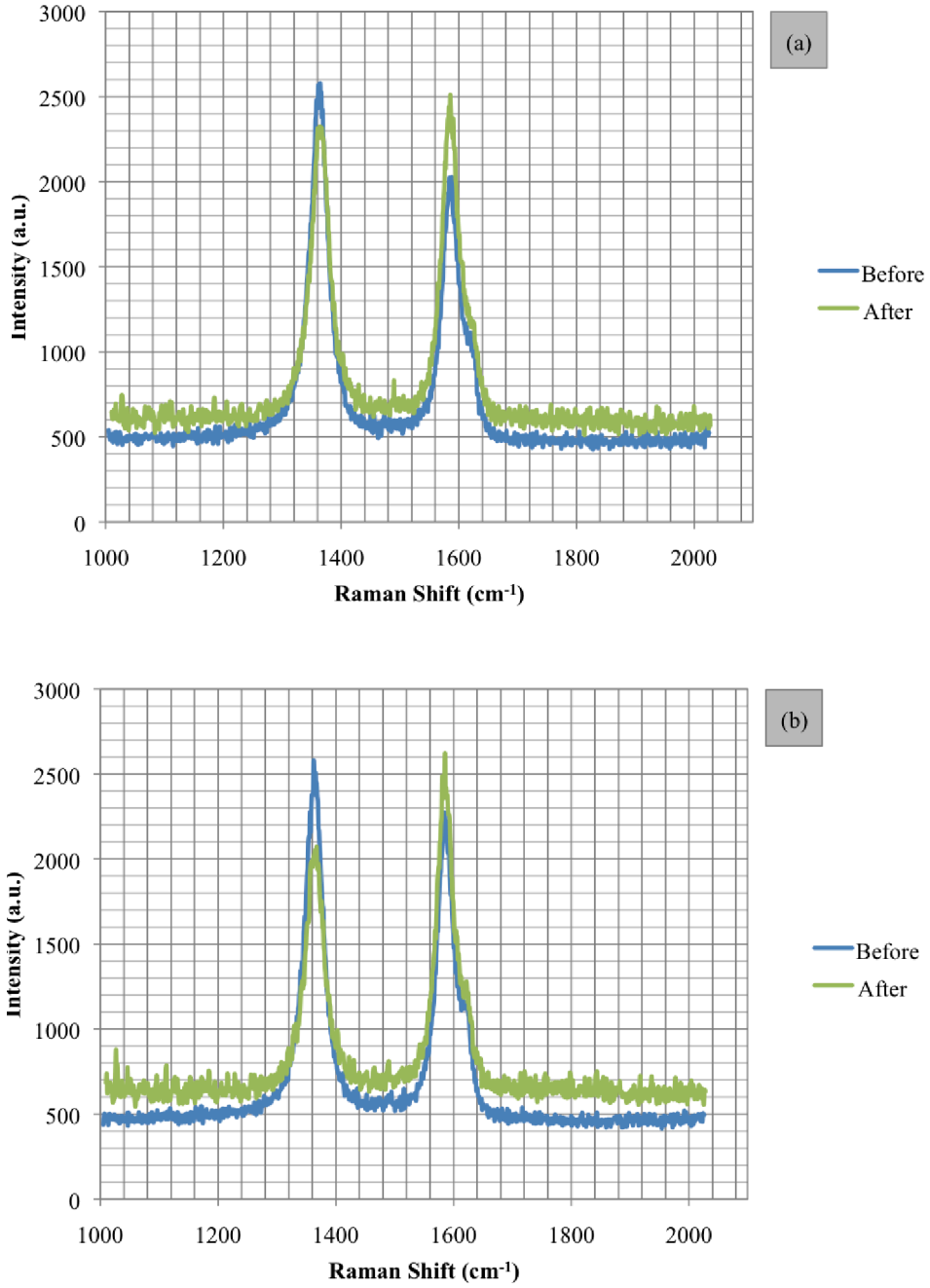

Figure 5. Raman spectra for CNT TIMs exposed to (a) 50 Mrad and (b) 100Mrad gamma radiation. Raman spectra before exposure also shown.

To determine the intensities of each peak, the acquired Raman spectra were analyzed by fitting them to a Breit-Wagner-Fano (BWF) spectral line shape [23]. This procedure removes uncertainty due to contributions from overlapping peaks in

determining the peak intensity. All samples before irradiation showed I_D/I_G ratios of ~1.3 which is higher than typical for MWCNTs [24] indicating significant presence of defects or edge effects resulting from the probing geometry used for the Raman measurement. After irradiation, samples subjected to a 50 Mrad dose exhibited a much lower I_D/I_G ratio of approximately 1.00; 100 Mrad samples showed a slightly lower ratio of approximately 0.95. The ratio of the D'-peak height to the G-peak height is also affected, but less markedly, changing from approximately 0.40 before irradiation to approximately 0.35 after irradiation for both doses. These changes result in a decrease of approximately 20% in the I_D/I_G ratios for both exposures and indicate that the I_D/I_G ratio is independent of gamma radiation dose, at least within the range of dosages tested. Figure 6 below summarizes these observations.

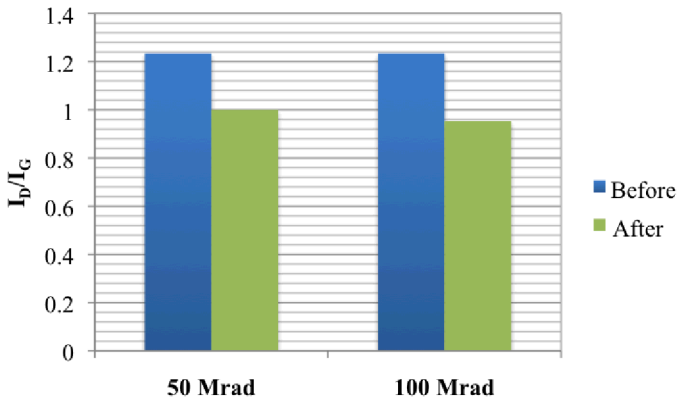

Figure 6. I_D to I_G band ratios for CNT TIMs before and after exposure to 50 and 100 Mrad.

The trends observed in Fig. 6 resemble those reported by Xu *et al*. [16] but contradict the trends reported by Guo *et al*. [15]. Thus, sp-3 hybridization does not occur in the tube structures in this work, and the increase in quality is most likely due to improved graphitic order within the tube walls [16]. The scatter in the reported results could be

attributed to the plethora of growth processes for CNT arrays that yield myriad tube structures.

The thermal resistances for six CNT TIMs were measured by the PA technique at a contact pressure 134 kPa and room temperature. Each of the CNT TIMs was tested before and after exposure. Figure 7 contains a plot of the thermal resistance values for the six CNT TIMs before and after exposure. The resistance values in the figure are averaged across three samples for each of the dosages. Based on the measurement uncertainty, the error associated with the thermal resistances is 1 mm^2 K/W. The thermal results indicate that exposure to gamma radiation dosages between 50 and 100 Mrad has no effect on thermal performance. The slight decreases in thermal resistance after exposure to both 50 and 100 Mrad are most likely due to the sequential process of thermal testing the CNT TIMs rather than CNT interaction with gamma radiation. The thermal results are encouraging because the performance did not degrade after exposure, indicating that the CNT TIMs can withstand gamma-ray irradiation without adverse thermal effects, at least within the range of 50 and 100 Mrad dosages.

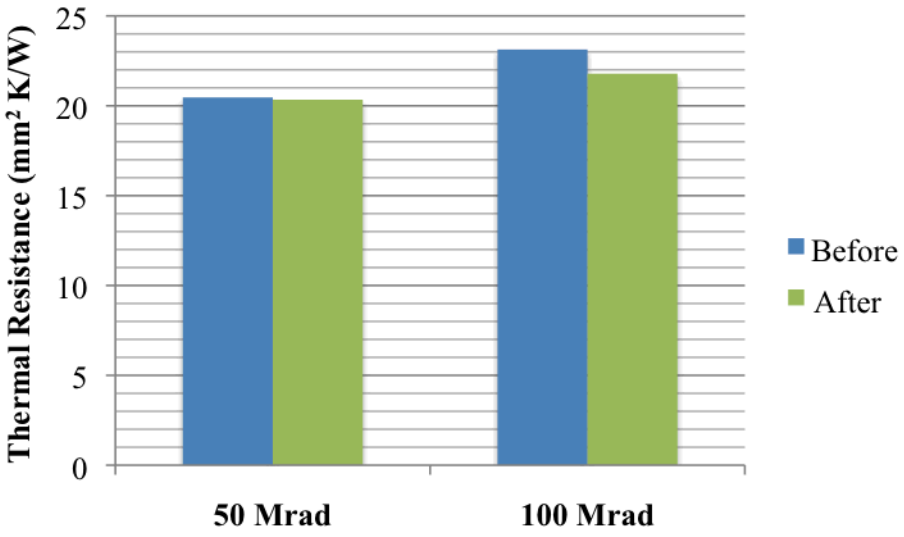

Figure 7. Thermal resistance for CNT TIMs before and after exposure to 50 and 100 Mrad. The opposing substrate was a 25 µm thick Ag foil. Thermal resistance values are averaged across three samples.

Conclusions

CNT-TIMs were exposed to gamma radiation in dosages of 50 and 100 Mrad. The quality of the CNTs, based on the I_D/I_G band ratio, was monitored by Raman spectroscopy and showed a moderate increase in the graphitic order of the CNT walls. Additionally, the thermal interface resistance was measured before and after gamma-ray irradiation using a transient photoacoustic method and while the exposure to such radiation has the potential to significantly affect CNT TIMs, no degradation in thermal performance was observed. Further studies such as thermal testing in a range of contact pressures coupled with nanoindentation experiments would help delineate the effects of gamma irradiation on the thermomechanical performance of CNTs.

Acknowledgment

Sandia National Laboratories is a multi-program laboratory managed and operated by Sandia Corporation, a wholly owned subsidiary of Lockheed Martin Corporation, for the U.S. Department of Energy's National Nuclear Security Administration under contract DE-AC04-94AL85000.

References

[1] International Technology Roadmap for Semiconductors (ITRS). *ITRS 2007 Edition*. http://www.itrs.net/Links/2007ITRS/Home2007.htm, 2007.

[2] R. Prasher, 2006, "Thermal Interface Materials: Historical Perspective, Status, and Future Directions," *Proceedings of the IEEE,* 94(8):1571, 2006.

[3] M. A. Panzer, G. Zhang, D. Mann, X. Hu, E. Pop, H. Dai, and K. E. Goodson, 2008, "Thermal Properties of Metal-Coated Vertically Aligned Single-Wall Nanotube Arrays," *J. of Heat Transfer*, 130, 052401.

[4] J. Xu and T. S. Fisher, 2006, "Enhanced Thermal Contact Conductance using Carbon Nanotube Array Interfaces," *IEEE Transactions on Components Packaging Technologies*, 29(2), pp 261-267.

[5] X. Hu, L. S. Pan, G. Gu, and K. E. Goodson, 2009, "Superior Thermal Interfaces Made by Metallically Anchored Carbon Nanotube Arrays ," *Proceedings of ASME Summer Heat Transfer Conference*, paper InterPACK2009-89375, San Francisco, CA.

[6] B. A. Cola, X. Xu, and T. S. Fisher, 2007, "Increased Real Contact in Thermal Interfaces: A Carbon Nanotube/foil Material," *Appl. Phys. Lett.*, 90, 093513.

[7] B. A. Cola, S. L. Hodson, X. Xu, and T. S. Fisher, 2008, "Carbon Nanotube Array Thermal Interfaces Enhanced with Paraffin Wax," *Proceedings of ASME Summer Heat Transfer Conference*, paper HT2008-56483, Jacksonville, FL.

[8] B. A. Cola, J. Xu, and T. S. Fisher, 2009, "Contact Mechanics and Thermal Conductance of Carbon Nanotube Array Interfaces," *Intl. J. of Heat and Mass Trans.*, 52, pp. 3490 – 3503.

[9] J. Wasniewski, D. Altman, S.L. Hodson, T.S. Fisher, A. Bulusu, S. Graham, B.A. Cola, "Characterization of metallically bonded carbon nanotube-based thermal interface materials using a high accuracy 1D steady state technique," Proceedings of the ASME 2011 Pacific Rim Technical Conference and Exhibition on Packaging and Integration of Electronic and Photonic Systems, MEMS and NEMS, Paper InterPACK2011-52148, 2011.

[10] M. Park, B. A. Cola, T. Siegmund, J. Xu, M. R. Maschmann, T. S. Fisher, and H. Kim, "Effects of Carbon Nanotube Array on Electrical Contact Resistance between Copper Substrates," *Nanotechnology*, 17:2294, 2006.

[11] Khare B., Meyyappan M., Moore M. H., Wilhite P., Imanaka H., and Chen B., 2003, "Proton Irradiation of Carbon Nanotubes," Nano Letters, **3**(5), pp. 643–646.

[12] Krasheninnikov A. V., and Nordlund K., 2004, "Irradiation effects in carbon nanotubes," Nuclear Instruments and Methods in Physics Research Section B: Beam Interactions with Materials and Atoms, **216**, pp. 355–366.

[13] Kis A., Csányi G., Salvetat J.-P., Lee T.-N., Couteau E., Kulik A. J., Benoit W., Brugger J., and Forró L., 2004, "Reinforcement of single-walled carbon nanotube bundles by intertube bridging.," Nature materials, **3**(3), pp. 153–157.

[14] Skákalová V., Hulman M., Fedorko P., Lukác P., and Roth S., 2003, "Effect Of Gamma-Irradiation on Single-Wall Carbon Nanotube Paper," AIP Conference Proceedings, AIP, pp. 143–147.

[15] Guo J., Li Y., Wu S., and Li W., 2005, “The effects of gamma-irradiation dose on chemical modification of multi-walled carbon nanotubes.,” Nanotechnology, **16**(10), pp. 2385–8.
[16] Xu Z., Chen L., Liu L., Wu X., and Chen L., 2011, “Structural changes in multi-walled carbon nanotubes caused by γ-ray irradiation,” Carbon, **49**(1), pp. 350–351.
[17] Miao M., Hawkins S. C., Cai J. Y., Gengenbach T. R., Knott R., and Huynh C. P., 2011, “Effect of gamma-irradiation on the mechanical properties of carbon nanotube yarns,” Carbon, **49**(14), pp. 4940–4947.
[18] M. R. Maschmann, P. B. Amama, A. Goyal, Z. Iqbal, R. Gat, and T. S. Fisher, 2006, “Parametric Study of Synthesis Conditions in Plasma-enhanced CVD of High-quality Single-walled Carbon Nanotubes,” *Carbon,* 44, pp. 10-18.
[19] Sayer R. A., Koehler T. P., Dalton S. M., Grasser T. W., and Akau R. L., 2013, “Thermal Contact Conductance of Radiation-Aged Thermal Interface Materials for Space Applications,” Proceedings of the ASME 2013 Summer Heat Transfer Conference, pp. HT2013–17408.
[20] B. A. Cola, J. Xu, C. Cheng, H. Hu, X. Xu, and T. S. Fisher, 2007, “Photoacoustic Characterization of Carbon Nanotube Array Interfaces,” *J. Appl. Phys.*, 101, 054313.
[21] Ferrari, A. C., and Robertson, J., 2004, "Raman Spectroscopy of Amorphous, Nanostructured, Diamond–Like Carbon, and Nanodiamond," Philosophical Transactions of the Royal Society of London. Series A: Mathematical, Physical and Engineering Sciences, 362(1824), pp. 2477-2512.
[22] Li, W., Zhang, H., Wang, C., Zhang, Y., Xu, L., Zhu, K., and Xie, S., 1997, "Raman Characterization of Aligned Carbon Nanotubes Produced by Thermal Decomposition of Hydrocarbon Vapor," Applied Physics Letters, 70(20), pp. 2684-2686.
[23] Brown, S. D. M., Jorio, A., Corio, P., Dresselhaus, M. S., Dresselhaus, G., Saito, R., and Kneipp, K., 2001, "Origin of the Breit-Wigner-Fano Lineshape of the Tangential G-Band Feature of Metallic Carbon Nanotubes," Physical Review B, 63(15), pp. 155414.
[24] Heise, H. M., Kuckuk, R., Ojha, A. K., Srivastava, A., Srivastava, V., and Asthana, B. P., 2009, "Characterisation of Carbonaceous Materials Using Raman Spectroscopy: A Comparison of Carbon Nanotube Filters, Single- and Multi-Walled Nanotubes, Graphitised Porous Carbon and Graphite," Journal of Raman Spectroscopy, 40(3), pp. 344-353.